

USES OF THE EXPERIMENTAL AREA OF A PROTON THERAPY FACILITY FOR BIOMEDICAL EXPERIMENTS

J. W. Kim* Research Institute and Hospital, National Cancer Center, Kyonggi, Korea

C. C. Yun, National Center for Inter-University Research Facility, Seoul National University, Seoul, Korea

Abstract

A biomedical beam line has been designed for the experimental area of the proton therapy facility based on a 230-MeV fixed-energy cyclotron. The beam line system is aimed to deliver sub-mm size beams in the energy range of 20-50 MeV, and is composed of an energy-degrader, slits and quadrupole magnets. Before the patient treatment began in March 2007, the experimental area had been used for measurements using a beam. We have performed a proton beam CT adopting the range modulation method to study the feasibility of proton radiography for use in patient positioning. In addition, we are developing a gamma detector system composed of a time projection chamber and a position sensitive scintillation array to locate the distal dose falloff in proton dose distribution by measuring prompt gamma distribution. Some results of the beam optics simulations and beam experiments are discussed.

INTRODUCTION

The National Cancer Center (NCC) in Korea has a proton therapy facility based on a 230-MeV cyclotron as shown in Fig.1 [1]. The cyclotron has an advantage as a medical accelerator in producing a stable cw beam adequate for the advanced radiation therapy using a scanning method. However, as its maximum energy is fixed, a lower energy beam is not readily available. The proton beam energy of below 50 MeV with the beam size in the range of a few mm to sub mm is useful in the fields of radiobiology and material science utilizing radiation [2]. The existing therapy facility with a new beam line for a low-energy and small-size beam is expected to accommodate diverse researches such as targeted irradiations on small biological objects and nuclear analysis.

A new beam line has been designed with extensive beam optics computations first for a simple configuration as described in ref. 3. In this article we present further results when a dipole magnet is added to select beam momentum as depicted in Fig. 1 to reduce the beam size at the focal point.

The experimental area has been used to develop quality assurance techniques helpful in proton therapy. One study is related to proton radiographs for use in patient positioning by improving the image resolution with helps

of Monte Carlo simulations. Secondly, we try to develop a gamma detection system to locate distal dose falloffs in situ. There are two kinds of methods in finding the location by measuring gammas emitted from nuclear reactions: one is to measure the prompt gammas emitted in the normal direction to the incident proton, and the other is to measure gammas emitted by the PET isotopes. We chose the former method, and have successfully correlated prompt gamma distributions to the locations of distal dose falloffs within 1-2 mm in the energy range of 100-200 MeV [4]. Further we are performing Monte Carlo simulations to develop a new gamma detection system, which can measure both the location and direction of a prompt gamma by coincidence between Compton-scattered electron and scattered gamma.

The first patient was treated in a gantry room in March this year. Then use of the experimental area has been difficult due to the concern of interference with clinical operations. Also, entering the area is currently not permitted while the treatment is underway, although it will be resolved soon. Meanwhile, we continue to experiment on the proton radiography and microbeam formation with a slit system, using a 40-MeV proton beam available at the Korea Cancer Center hospital in Seoul.

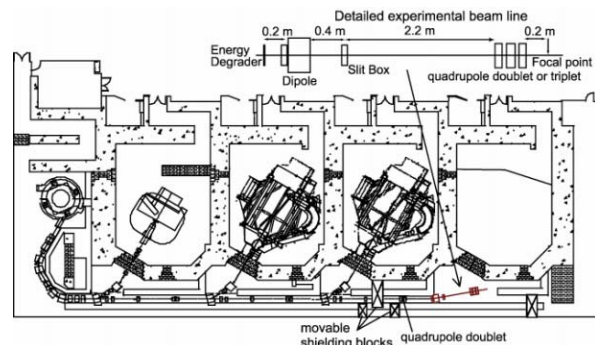


Figure 1: View of the proton therapy facility at the NCC. The beam line designed for the experimental area is magnified.

BEAM LINE DESIGN

The design of a proton beam line for the experimental area was carried out using TRANSPORT and TURTLE programs [5]. This beam line consists of an energy degrader, two slits, and three quadrupole magnets [3].

* This work is supported by a grant from National Cancer Centre.

The degrader made of acryl has been tested using a 100-MeV beam, but we plan to use graphite for the final degrader. The quadrupoles are in the possession with an effective length of 22 cm, having a maximum focusing gradient of 14 T/m in the clear bore diameter of 65 mm.

Figure 2 shows beam emittance growths when a graphite degrader reduces the incident proton beam energy from 100 MeV to 50 and 20 MeV, respectively. A rapid increase in transverse emittance is clearly seen. A new program was written for beam transport inside the degrader by adapting routines imbedded in the code INTENSITY developed by a nuclear physics group [6]. A Gaussian beam is initially assumed, and a total of twenty thousand particles are used for typical simulations, and up to 1.6×10^6 particles for the cases of using narrow slits.

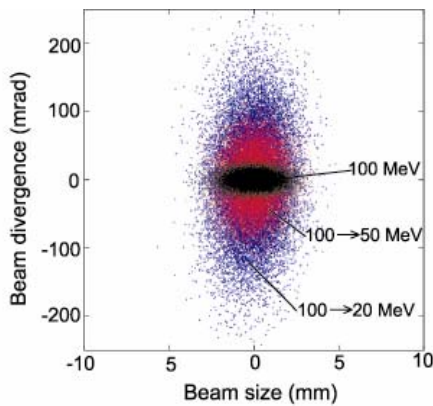


Figure 2: Transverse phase spaces at the entrance (black) and the exit of the degrader when the beam energy is degraded to 50 MeV (red) or 20 MeV (blue)

Figure 3 shows the beam envelopes when the beam energy is degraded to 50 MeV from 100 MeV. This is a case when a 10° dipole magnet with a bending radius of 2 m is used to select beam momentum in the downstream of the degrader. The first slit is designed to cut off the major part of the phase space eventually to be removed by the second slit, allowing the second to make a fine selection. This arrangement as also shown in Fig. 1 helps in reducing neutron background at the final focus.

A comparison of phase spaces at the final focus with and without a dipole magnet is made in Fig. 4. Without the dipole the chromatic error strongly affects the vertical focusing as shown as a bow-tie shape in the phase space. On the other hand momentum selection by a dipole significantly decreases chromatic aberration so as to reduce the focused beam size. The current optics study showed that a larger dispersion by a dipole with more than 10° bending tends to distort the horizontal phase space.

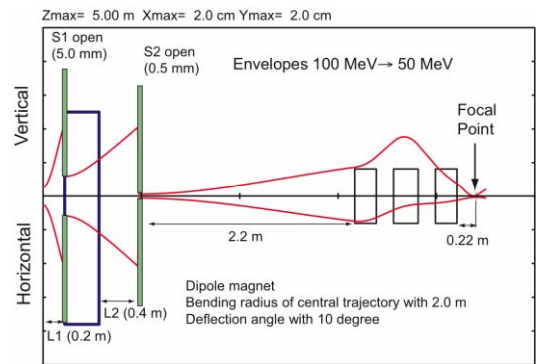


Figure 3: Beam envelopes in the new beam line calculated by TURTLE for the case of using a dipole magnet.

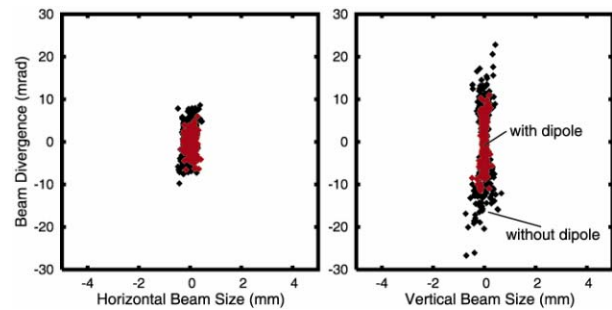


Figure 4: Transverse phase spaces at the focal point without a dipole (black) and with a dipole magnet (red) located between S1 and S2 slits.

The beam size at the focal point with and without a dipole magnet is plotted in Fig. 5. The beam size with a dipole is smaller than 0.2 mm at the focal point in both horizontal and vertical planes when S2 opening is 0.5 mm. However, this is at the cost of transmission efficiency as it is reduced by half.

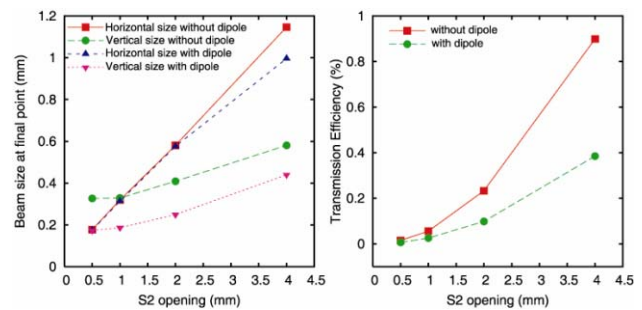


Figure 5: Reduction of the final-focused beam size and transmission efficiency plotted as a function of S2 opening for the cases of with and without a dipole magnet.

USES OF EXPERIMENTAL AREA

The proton beam energy of 230-MeV is currently the highest available in Korea. As the experimental area is part of the therapy facility, we try to focus on researches related to proton therapy. The accuracy of patient

positioning in particle therapy is more critical than for conventional photon therapy because its dose distribution is more sharply defined. The usual x-ray portal image system has two sets of x-ray generator and flat panel displays to ensure the patient position, and may have some disadvantage in performing regular alignment with the proton beam.

A proton CT system was tested as shown in Fig. 6. The proton radiography is performed using a range modulated proton beam [7] and a CCD camera-scintillation system [8]. The modulator designed by Monte Carlo simulations rotates at over 5 Hz to make the dose distribution monotonically decreasing in depth. A phantom is positioned on a turntable, so that a series of projection images can be attained to reconstruct the CT image. An acryl phantom and its image are shown also in Fig. 6. We are currently working on the way to improve both the spatial and density resolutions thru experiments using a 40-MeV proton beam and Monte Carlo simulations.

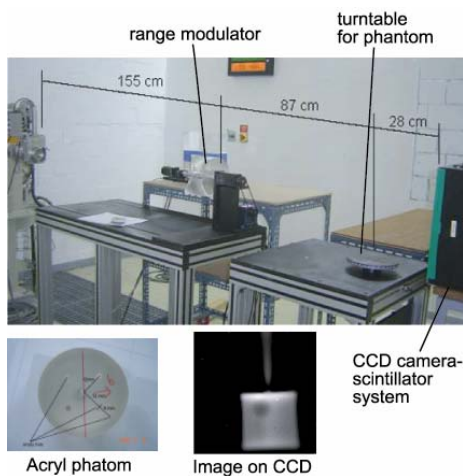


Figure 6: Upper: Arrangement of the proton radiography system. Lower: an acryl phantom with a few inserts and its image by proton radiography.

The proton beam therapy has a clear advantage in distal dose falloff as the dose beyond the range almost doesn't exist. However, there is some uncertainty in the range computed from the X-ray CT images. We are developing a system, which can measure the falloff location in situ.

The previous measurement system we developed consists of a collimation system composed of three layers of shielding and a CsI scintillation detector [4] as shown in Fig. 7. The system has to be moved to scan the gamma intensity near the falloff location, which makes the system inadequate for the moving beam. We are now developing a new stationary system to measure both the location and direction of the gamma by tracking Compton-scattered electron and gamma coincidentally, much like the Compton camera system. Monte Carlo simulations have been performed to optimise the system, and preparation for the test is underway.



Figure 7: A setup to measure the prompt gamma distributions. Water phantom and the collimator system are shown. The CsI detector is taken out to count background radiation.

SUMMARY

The experimental area of the proton therapy facility can be utilized to perform biomedical experiments and to develop quality assurance techniques for particle beam therapy. A new beam line for the area has been designed, and we are now testing a slit system to produce microbeams at a 50-MeV cyclotron facility. The area has been used to study on proton radiography for potential use in patient positioning by improving the image resolution. In addition we have measured the correlation between the distal dose falloff and prompt gamma distribution within 1-2 mm. Now a series of Monte Carlo simulations with GEANT3 is underway to design a new gamma detection system for measuring both the initial location and direction of the prompt gamma. An actual system will be assembled and tested soon.

REFERENCES

- [1] J. Kim, J. Korean Phys. Soc. 43 (2003) S50.
- [2] G. Datzmann, et. al. Nucl. Instr. and Meth. B181 (2001) 20.
- [3] C. Yun, J. Kim, Nucl. Instr. and Meth. B (2007) in press.
- [4] C. Min, C. Kim, M. Youn, J. Kim, App. Phys. Lett. 89, 183517 (2006).
- [5] PSI Transport/TURTLE by U. Rohrer based on CERN-SLAC-FERMILAB version by K.L. Brown et al.
- [6] J.A. Winger and B.M. Sherrill, D.J. Morrissey, Nucl. Instr. and Meth. B70 (1992) 380.
- [7] P. Zygmanski, et. al., Phys. Med. Biol. 45 (2000) 511.
- [8] J. Kim, et. al., Japan. J. of App. Phys., 45 (2006) 5297.